Pyrazole Amides Towards Trailblazing Antimicrobial Research: Bridging in Vivo Insights and Molecular Docking Studies

Khandekar Mangala[1,2], Choudhary Aasiya[1,2], Varsha Naikwadi[1], Vikram Gaikwad[1], Tanaji Jadhav[1], DVRN Bhikshapathi[3], Mahesh Palled[4], Aravind Karadi[5], Ravindra Kulkarni[6]

[1]*Department of Pharmaceutical Chemistry, SVERIs College of Pharmacy, Gopalpur, India;*
[2]*Department of Pharmaceutical Chemistry, Punyashlok Ahilyadevi Holkar Solapur University, Solapur, India*
[3]*Department of Pharmaceutics, Teegala Ram Reddy College of Pharmacy, Meerpet, Balapur (M), Hyderabad, 500 059*
[4]*Department of Pharmaceutical Chemistry, KLEs College of Pharmacy, JNMC Campus, Nehru Nagar, Belagavi India – 590010*
[5]*Hkes Matoshree Taradevi Rampure institutes of pharmaceutical sciences sedam Road kalaburagi Karnataka*
[6]*Department of Pharmaceutical Chemistry, BVDU's Poona College of Pharmacy, Pune, India.*
Email: ravigk2000@gmail.com
Corresponding Author: Ravindra Kulkarni

KEYWORDS
Pyrazole amides, Anti-Tubercular, Antibacterial, Antifungal, Molecular Docking studies.

ABSTRACT

Antimicrobial resistance presents a significant threat to contemporary healthcare systems, making it increasingly difficult to treat infections that were once easily managed. This study aims to assess the efficacy of pyrazole benzamide derivatives (M5a–M5o), which were synthesized for their antimicrobial and antifungal activities. These compounds were tested against methicillin resistant staphylococcus aureus (MRSA), vancomycin resistant staphylococcus aureus (VRSA), mycobacterium tuberculosis H37Rv and other resistant species. The minimum inhibitory concentrations (MIC) were determined using standardized protocols to evaluate their potency and effectiveness. Molecular docking studies were also conducted to explore potential interactions and binding affinities at the molecular level, providing further insights into their antimicrobial and anti-tubercular mechanisms. Compounds M5i, M5k, and M5b emerged as the most potent, displaying MIC value of 3.12 µg/ml. These compounds show great potential as new agents in addressing the growing problem of antimicrobial resistance. Molecular docking studies against Enoyl-[acyl-carrier-protein] reductase (4DRE), revealed key interactions, with compound M5n showing a docking energy of -9.8 kcal/mol and compound M5g at -9.6 kcal/mol. These compounds formed important hydrogen bonds and π-interactions with residues like Lys165, Gly14, Ser94, and Ile21. Overall, the findings indicate that specific pyrazole-benzamide derivatives exhibit promising antimicrobial and antifungal activities, underscoring their potential as therapeutic agents. Additionally, the integration of molecular docking studies proves valuable in guiding the development and optimization of these compounds for future therapeutic applications.

1. Introduction

The rise of antimicrobial resistance in microorganisms is a significant global public health concern. One of the leading contributors to increased mortality rates is the declining effectiveness of existing pharmaceuticals in treating infections caused by these resistant strains [1]. Clinically approved antibiotics and antimicrobial agents have traditionally been successful in either inhibiting the growth of microbes or eradicating them entirely. However, the quest for new, effective therapies has become increasingly urgent and challenging [2]. Well known drug resistant strains, such as vancomycin resistant staphylococcus aureus (VRSA), vancomycin resistant enterococci (VRE), methicillin resistant staphylococcus aureus (MRSA), certain strains of E. coli, and bacteria carrying Carbapenemase genes, have developed resistance to most currently available antibacterial agents [3,4]. Tuberculosis (TB), a highly contagious disease, remains a critical global health issue and a leading cause of death worldwide. Before the COVID-19 pandemic, TB was the leading cause of global mortality. According to the World Health Organization's 2022 Global Tuberculosis Report, TB caused 1.6 million deaths in 2021, including 1.4 million deaths among HIV-negative individuals and 187,000 among HIV positive individuals. Additionally, 10.6 million new TB cases were diagnosed in 2021, with 450,000 being rifampicin resistant TB (RR-TB), further compounding the challenge of drug resistant TB (DR-TB). From 2020 to 2021, the global incidence of TB increased by 3.6% [5]. The growing prevalence of multi-drug-resistant (MDR) and extensively drug-resistant (XDR) strains threatens global efforts to control TB. As Mycobacterium tuberculosis (Mtb) acquires resistance to first and secondline drugs, access to key medications like isoniazid (INH) and rifampicin is increasingly limited [6]. A deeper understanding of new drug targets and mechanisms of resistance is crucial for developing next generation anti-TB therapies. Current TB treatment regimens involve a range of drugs, including isoniazid, ethionamide, rifampicin, ethambutol, and fluoroquinolones [7-9].

Pyrazole and its derivatives play a pivotal role in medicinal and agrochemical research due to their wide range of biological activities, including anti-inflammatory, antidepressant, anticonvulsant, antihyperglycemic, antipyretic, antibacterial, antifungal, antiproliferative, anti-HIV, antimicrobial, and anti-tubercular properties [10]. The literature highlights that compounds containing a pyrazole core demonstrated potent antimicrobial and anti-tubercular activity, even against resistant strains. The structural diversity and promising biological activities of N-pyrazolyl benzamide derivatives have garnered significant interest in the search for novel therapeutic agents [9,11-15].

Akula G. (2018) investigated the structure activity relationships of N-pyrazolyl benzamide derivatives, identifying critical modifications that markedly improved their antibacterial effectiveness [14]. Similarly, Kulkarni et al. (2014) demonstrated that N-pyrazolyl benzamides possess strong antibacterial activity against both gram-positive and gram-negative bacteria, with certain compounds showing minimum inhibitory concentration (MIC) values as low as 0.5 µg/ml. The study further indicated that incorporating electron-withdrawing groups on the pyrazole ring significantly enhanced the antibacterial potency of these derivatives [13].

In our previous research, the synthesis of a series of pyrazole benzamides, designated as compounds M5a to M5o, and evaluated their potential for anti-inflammatory activities. Building on these initial results, the current study focuses on investigating the antimicrobial properties of these compounds through both in vitro experiments and molecular docking analyses. The objective of the present paper is to study the antimicrobial spectrum including effectiveness against Mtb, fungal strains, normal bacterial strains, and resistant strains. In addition to the in vitro antimicrobial studies, study also conducted molecular docking analysis to examine the interactions between these compounds and enzyme involved in cell wall synthesis. This computational method will provide insights into the binding affinity of the compounds and their potential putative molecular target of action, offering a deeper understanding of their therapeutic potential.

2. Materials and methods

A six stage reaction station from Radleys was used for all reactions. Synthetic grade chemicals were sourced from Sigma Aldrich and local vendors without purification. Reaction progress was tracked on TLC plates with iodine vapors and UV light. Melting points were measured using a Remi apparatus, and column chromatography employed 60-120 mesh silica gel. IR spectra were recorded on Agilent FTIR, ^{1}H NMR scans on BRUKER DRX 500 MHz with TMS as the standard, and mass data on Agilent ESI MS.

2.1 Chemistry

This scheme outlines the synthesis of compound M5a-o, which has been evaluated for anti-inflammatory activity and simulation studies elsewhere. Hence a concise methodology of synthesis is provided here. The synthesis of 4-bromophenylhydrazine hydrochloride begins with the diazotization of 4-bromoaniline (0.01 mol) using HCl and sodium nitrite at 0 °C, followed by reduction with stannous chloride in HCl, stirring for 1 hour, and overnight refrigeration. The product is then neutralized with KOH, extracted in ether, dried, and treated with HCl gas (Scheme 1) [16]. For 5-Amino-1-(Substituted) phenyl-3-t-butyl pyrazole (3a-b), 4,4-dimethyl-3-oxo-pentanenitrile and substitute phenylhydrazine hydrochlorides are refluxed in ethanol with AcOH overnight, followed by washing, organic extraction, and solvent evaporation. The final synthesis of N-[3'-t-Butyl-1'-(Substituted) phenyl pyrazol-5'-yl] benzamides (M5a-o) involved stirring the pyrazole derivative with triethylamine and benzoyl chloride in DCM, followed by washing, drying, and purification over silica (Scheme 2) [17, 12].

Scheme 1: Synthetic Pathway for 4-bromophenylhydrazine hydrochloride.

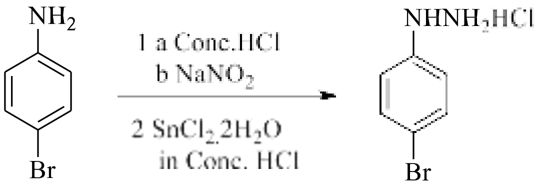

Scheme 2: Synthetic Pathway for N-Substituted Benzamides.

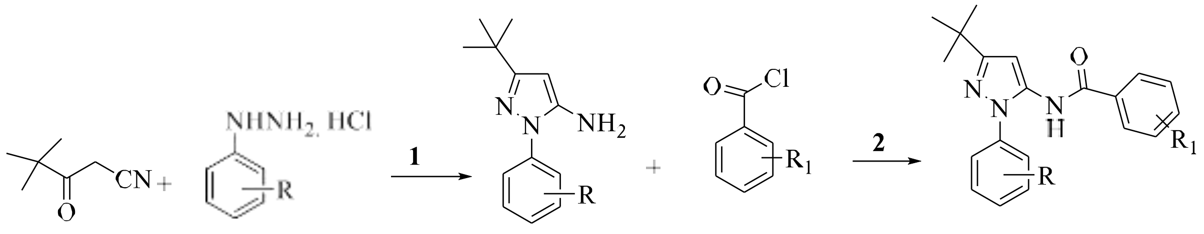

M1

M2a-b
a=4-Br
b=3-CH_3

M3a-b
a=4-Br
b=3-CH_3

M4a-j

a=H	f=4-F
b=4-CH_3	g=3-F
c=4-Cl	h=2-F
d=3-Cl	i=4-NO_2
e=2-Cl	j=3-NO_2

M5a-o

1 Abs EtOH, reflux over night
2 TEA/Pyridine /DIPEA,DCM,RT

2.2 Antimicrobial Activities

All the synthesized compounds 5Ma-o have been tested for their potential antimicrobial activities consisting of wild type organisms Bacillus subtilis, Staphylococcus aureus, Klebsiella pneumonia, E. coli, Aspergillus flavus, Candida albican and mycobacterium tuberculosis H_{37}Rv. Apart from the afore listed wild types, molecules have been tested against mutant strains consisting of MRSA (ATCC43300), VRSA (S101) and Escherichia Faecium (CCX48585).

2.2.1 Preparation of Test Samples and Determination of MIC

A stock solution of 5Ma-o in DMSO was prepared at a concentration of 100 µg/mL. A serial dilution of each compound was prepared with resultant concentrations of (100, 50, 25, 12.5, 6.25, 3.12, 1.6, and 0.8 µg/mL) by diluting with water. These dilutions were utilized for the estimation of the MIC of the respective compounds [18].

2.2 Antimicrobial Activity (Antibacterial and Antifungal)

The antimicrobial activity estimation of the synthesized compounds was carried out utilizing Muller Hinton broth as per the instructions outlined in document M27-A 2015 (in CLSI). The estimation utilized overnight cultures of Bacillus subtilis, Staphylococcus aureus, Klebsiella pneumoniae, E. coli strains, Aspergillus flavus, as well as Candida albicans strains. The dilutions prepared as the test samples above were added to culture plates containing microbial cultures of respective organisms and further incubated at appropriate temperatures. The cultures were then observed for visible growth or inhibition which indicates the compound's antimicrobial effectiveness and the results are recorded as minimum inhibitory concentration [14, 19, 20].

2.3 Anti-tubercular Assay

2.3.1 Test Organisms and Preparation of Inoculum

The in vitro anti-tubercular activity of the synthesized compounds was assessed against the Mtb H37Rv (ATCC 27294) strain, susceptible to Isoniazid. The bacterial strain underwent sub-culturing at 37°C for two weeks, being supplied with Muller Hinton broth to generate a fresh batch of strain for the study. Bacterial suspensions were prepared by diluting with a normal saline solution with 0.5 Mc Farland standard turbidity, equivalent to 108 CFU. The mixture was vortexed for 30 seconds in a glass vessel, and the particles were allowed to settle. For inoculation 100 µL of the microbial suspension was used. The lowest concentration at which there is no growth of the bacterium was observed and recorded [21, 22,].

2.4 Molecular Docking

A detailed molecular docking study was performed to clarify the interactions between ligands and the amino acids in the active site and determine favorable conformations for stable docking complexes. The Vina module of AutoDock, a well known computational tool for modelling the binding interactions between small compounds and biological macromolecules, was used to perform molecular docking research [23].

The basis for the docking studies was the protein target's three-dimensional structure, which was acquired from the RCSB Protein Data Bank (PDB ID: 4DRE). The atomic co-ordinates of the protein were precisely represented by the high-resolution X-ray crystallographic data, which made it possible to simulate the binding site and any interactions with accuracy.

ChemDraw 14.0 is a versatile molecular drawing program that was used to thoroughly design the chemical structures of the potential ligands under examination. These ligand structures were then put through a rigorous preparation process that included energy optimization and minimization. The ChemDraw Bio 3D tools and AutoDock utilities made this process easier and ensured that the ligand structures were suitable for the docking simulations. Using AutoDock's specialized algorithms, protein preparation—a critical stage in molecular docking—was carried out, ensuring appropriate handling of the macromolecular structure and its possible binding sites. Then both ligand and protein save as. pdbqt by using AutoDock tools. Next, using AutoDock Vina 4.2, the molecular docking simulations were carried out while following industry best practices and established standards, with grid points set to center_x = -27.700, center_y = 15.522, and center_z = -9.208 [24]. In computational chemistry, the standard unit of measurement used to represent the binding affinities and energetics of molecular interactions is Kcal/mol, which was used to quantify the interaction efficiency of the compounds with the macromolecular target. These numbers, which were taken from the log files created throughout the simulation experiments, offer important information on the relative stabilities and strengths of the docking complexes that were established.

PyMOL 2.1.1 and Discovery Studio Visualizer 2020 are two potent molecular visualization tools that were used to visualize and analyze the spatial configurations and intermolecular interactions inside the docking complexes. With the use of these instruments, the three-dimensional structures could be thoroughly examined, allowing for the identification of crucial interactions that support the stability and specificity of the docking complexes. These interactions included hydrophobic interactions and hydrogen bonding [25, 26]. Such visualizations are instrumental in furthering our understanding of the mechanisms of action of the ligands and guiding future optimization efforts.

3. Results and discussion:

3.1 Anti-bacterial and antifungal activity

All fifteen molecules were attempted for the evaluation of their potential antibacterial and antifungal activity against various strains including Bacillus subtilis (MTCC 619), Staphylococcus aureus (ATCC 29213), gram-positive organisms, and Klebsiella pneumonia (MTCC 7162), Escherichia coli (MTCC 7162) gram-negative organisms. Moreover, Aspergillus flavus (MTCC 870), Candida albicans (MTCC 183), Methicillin-resistant Staphylococcus aureus (MRSA, ATCC 43300), Vancomycin-resistant Staphylococcus aureus (VRSA, S 101), Linezolid-resistant E. Faecium CC-X48585 were included for evaluation. Streptomycin was used against gram-positive organisms, tetracycline against gram-negative organisms, and fluconazole against fungal strains. All synthesized fifteen molecules have provided comprehensive insights into their antibacterial and antifungal activities in the range from 3.12 µg/ml to 100 µg/ml concentration as listed in table 1.

Table 1: MIC of pyrazole derivatives M5a-o against bacterial and fungal strains.

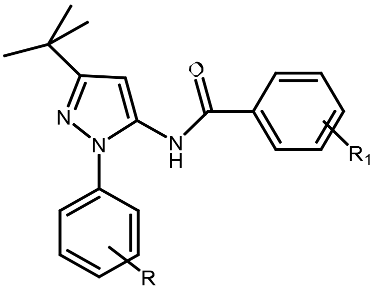

CODE	R	R1	Antimicrobial activity				Antifungal	
			BS*	SA*	KP*	EC*	AF*	CA*
M5a	4-Br	H	50	25	100	50	50	100
M5b	4-Br	4-CH_3	6.25	6.25	12.5	12.5	25	25
M5c	4-Br	4-Cl	25	25	50	50	100	50
M5d	4-Br	3-Cl	12.5	12.5	25	25	25	25
M5e	4-Br	2-Cl	25	25	50	50	3.12	6.25
M5f	4-Br	4-F	12.5	12.5	25	12.5	12.5	25

M5g	3-CH_3	4-CH_3	25	25	>100	>100	25	25
M5h	3-CH_3	4-Br	50	50	100	100	50	50
M5i	3-CH_3	3-Br	3.12	6.25	25	25	25	25
M5j	3-CH_3	2-Br	100	100	100	100	50	100
M5k	3-CH_3	2-F	50	25	100	100	100	100
M5l	3-CH_3	2-CF_3	50	25	50	50	25	25
M5m	3-CH_3	2-Cl	25	50	25	100	12.5	25
M5n	3-CH_3	3-NO_2	12.5	12.5	6.25	25	100	100
M5o	3-CH_3	3-NH_2	50	50	100	100	25	25
5w	3-CH_3	4-H	0.4	0.8	12.5	12.5	25	25
Streptomycin			50	50	>100	>100	>100	>100
Tetracycline			>100	>100	50	50	>100	>100
Fluconazole			>100	>100	>100	>100	50	50

BS: Bacillus subtilis; SA: Staphylococcus aureus, KP: Klebsiella pneumoniae;

EC: E. coli, AF: Aspergillus flavus, CA: Candidaalbican.

Table 2. MIC of pyrazole derivatives M5a-o against multi-drug resistant and MTB strains.

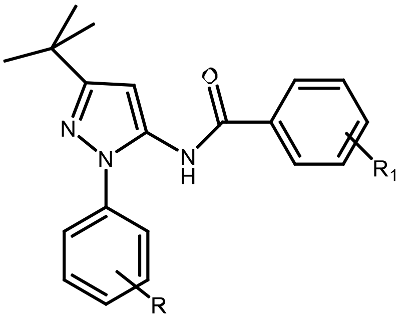

Code	R	R1	MRSA ATCC43300	VRSA S 101	E. Faecium CC-X48585	MTB H37Rv
M5a	4-Br	H	NA	NA	NA	100
M5b	4-Br	4-CH_3	12.5	12.5	25	6.25
M5c	4-Br	4-Cl	50	50	50	50
M5d	4-Br	3-Cl	6.25	12.5	12.5	25
M5e	4-Br	2-Cl	25	25	25	25
M5f	4-Br	4-F	12.5	25	25	12.5
M5g	3-CH_3	4-CH_3	25	25	25	50
M5h	3-CH3	4-Br	NA	NA	NA	50
M5i	3-CH3	3-Br	50	50	25	6.25
M5j	3-CH_3	2-Br	NA	NA	NA	25
M5k	3-CH_3	2-F	3.12	6.25	25	NA
M5l	3-CH_3	2-CF_3	50	50	100	12.5
M5m	3-CH_3	2-Cl	25	50	100	25
M5n	3-CH_3	3-NO_2	12.5	12.5	6.25	6.25
M5o	3-CH_3	3-NH_2	NA	NA	NA	12.5
5w	3-CH3*	4-H	6.25	3.12	6.25	25
Isoniazide		--	--	--	--	0.36
Pyrazinamide		--	--	--	--	30

* Reported compound

Among the fifteen compounds, four compounds displayed potent antimicrobial activity, M5i, M5b, M5n, and M5e. The synthesized molecule M5a (R= 4Br, R1= H) displayed moderate activity against Staphylococcus aureus (MIC: 25 µg/ml) and equipotent activity against Bacillus subtilis, Escherichia coli, and Aspergillus flavus (MIC: 50 µg/ml). However, it exhibited significantly lower activity against Klebsiella pneumonia (MIC: 100 µg/ml). Out of the four, three compounds M5i, M5b, and M5n displayed potent antimicrobial activity and M5e displayed potent antifungal activity with MIC - 3.12 µg/ml besides 6.25 µg/ml as listed in Table 1. Compounds M5i and M5b exhibited potent activity against the gram-positive strain Bacillus subtilis through MIC -3.12 µg/ml and 6.25 µg/ml, separately. The compound M5n demonstrated excellent antimicrobial activity against the gram-negative Klebsiella pneumonia signifying a MIC - 6.25 µg/ml. Compound M5e showed excellent antifungal activity against Aspergillus flavus indicating MIC - 3.12 µg/ml. The same compound exhibited potent antifungal activity against Candida albicans demonstrating a MIC - 6.25 µg/ml. While synthesized molecule M5b (R= 4Br, R1= 4CH_3) showed potent action against Bacillus subtilis as well as Staphylococcus aureus - signifying MIC: 6.25 µg/ml and better activity against Klebsiella pneumonia as well as E. coli (MIC: 12.5

µg/ml), demonstrating a 3-4-fold increase in antimicrobial activity compared to M5a. M5b also displayed moderate antifungal activity against Aspergillus flavus and Candida albicans (MIC: 25 µg/ml).

Chloro-substituted compounds M5e (R1= 2Cl), M5d (R1= 3Cl), and M5c (R1= 4Cl), M5e exhibits notable potent antifungal activity against Aspergillus flavus and Candida albicans signifying MIC - 3.12 µg/ml as well as 6.25 µg/ml concentration individually. M5d showed good antimicrobial activity against gram-positive strains Bacillus subtilis as well as Staphylococcus aureus demonstrating MIC - 12.5 µg/ml concentrations. Compounds M5e, M5d, and M5c displayed moderate activity against the remaining strains, with MIC values ranging from 25 to 50 µg/ml concentration while M5c is less active against Aspergillus flavus with a MIC value of 100 µg/ml concentration.

M5f (R= 4Br, R1= 4F) exhibited very good antimicrobial and antifungal activity against all strains indicating a MIC - 12.5 µg/ml concentration except against Klebsiella pneumonia as well as Candida albicans and showed moderate antifungal action signifying a MIC 25 µg/ml concentration. M5f is equipotent in activity to 5w against E. Coli that gram-negative strain. Amongst series M5a-f, ortho-substituted chlorine at R1 (M5e) is the most potent antifungal agent and methyl substitution at R1 (M5b) is the most potent antibacterial agent.

In the series of M5g-o, the molecule M5i (R= 3-CH_3, R1= 3-Br) exhibited potent antimicrobial activity against gram-positive strains Bacillus subtilis and Staphylococcus aureus demonstrating MIC of 3.12 µg/ml as well as 6.25 µg/ml correspondingly. Compound M5h (R= 3-CH_3, R1= 4-Br) exhibited equipotent activity against gram-positive strains and antifungal strains indicating MIC - 50 µg/ml. Compound M5g (R=3-CH_3, R1=4-CH_3) displayed moderate antimicrobial activity and antifungal activity (MIC: 25 µg/ml). Compound M5k and M5l displayed moderate efficacy against the gram-positive bacterium Staphylococcus aureus, revealing MIC values at 25 µg/ml concentrations. Additionally, M5l exhibited antifungal activity against Aspergillus flavus and Candida albicans, demonstrating MIC values at 25 µg/ml concentrations. Table 1 further shows the effectiveness of meta-substituted fluorine at R1 as seen in M5n (R= 3-CH_3, R1=3-NO_2), displaying potent antibacterial activity, suggesting MIC 6.25 µg/ml against Klebsiella pneumoniae as well as against Staphylococcus aureus MIC - 12.5 µg/ml. Compound M5m (R=3CH3, R1=4F) exhibits effective antifungal activity signifying a MIC 12.5 µg/ml against Aspergillus flavus. Compound M5n displayed potent antimicrobial activity against the gram-positive strain Klebsiella Pneumonia representing MIC - 6.25 µg/ml in comparison to 5w. Likewise, M5e exhibited potent antifungal activity against Aspergillus flavus (MIC: 3.12 µg/ml) and Candida albicans (MIC: 6.25 µg/ml) when compared to 5w.

Table 2 presents MIC values for compounds against various microbial-resistant strains and Mtb. All compounds displayed varying MIC values against all the strains in the range from 3.12 to 100 µg/ml. In the framework of MRSA, all compounds M5d and M5k exhibited potent antimicrobial activity indicating MIC - 3.12 µg/ml as well as 6.25 µg/ml respectively. Compounds M5b, M5f, then M5n exhibited good antimicrobial potential against MRSA with signifying MIC - 12.5 µg/ml. Remaining all compounds M5c, M5e, M5f, M5g, M5i, M5l, and M5m exhibited varying MIC values against MRSA. Against VRSA Strain S 101, amongst all compounds, M5k exhibited potent antimicrobial action demonstrating MIC - 6.25 µg/ml. Derivatives M5b, and M5d, besides M5n, exhibited good antimicrobial action against VRSA demonstrating MIC - of 12.5 µg/ml. Remaining all compounds M5c, M5e, M5f, M5g, M5i, M5l, and M5m exhibited varying MIC value against VRSA. In the framework of E. Faecium CC-X48585 amongst all compounds, only M5n exhibited potent antimicrobial potential indicating MIC 6.25 µg/ml. Derivative M5d exhibited good antimicrobial action against E. Faecium signifying MIC - 12.5 µg/ml and other molecules were less potent than M5n.

Against Mycobacterium tuberculosis H37Rv, amongst all compounds three compounds M5b, M5i, and M5n exhibited potent antimicrobial action indicating MIC - 6.25 µg/ml. The compounds M5f, M5l, and M5o exhibited potent antimicrobial potential representing MIC of 12.5 µg/ml, also remaining molecules exhibited varying MIC values against MTB H37Rv. As such no antibacterial compounds bearing pyrazole scaffold are available during the study, 5w (R= 3-CH_3) has been considered as another internal standard for comparison which showed potent antimicrobial effectiveness against VRSA S101 representing MIC - 3.12 µg/ml as well as MIC - 6.25µg/ml against MRSA and E. faecium. None of the synthesized compounds have matched these results against VRSA S101.

3.2 Molecular Docking Study

Enoyl-[acyl-carrier-protein] reductase [NADH] - (4DRE)

The NAI i.e. the co-crystallized ligand interacted with 4DRE in the hinge region and developed a hydrogen interaction with Gly14, Ile21, Ala22, Thr39, Leu63, Gly96, Lys165 and Ile194 as shown in Figure 1. Further to validate the docking protocol the co-crystallized ligand was redocked as shown in Figure 2.

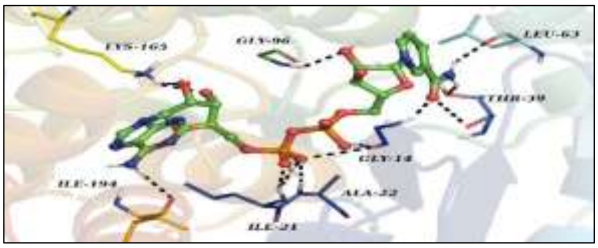

Figure 1: NAI (Co-crystal ligand) in complexed with 4DRE

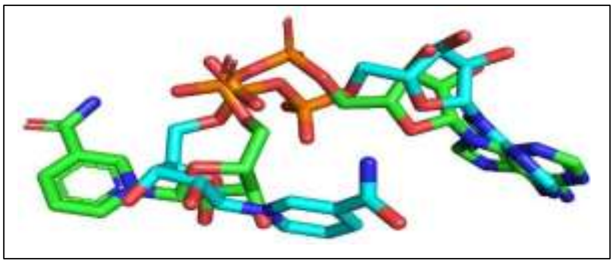

Figure 2: Alignment of co-crystallized ligand (green) and redocked co-crystallized ligand (blue) RMSD: 2.16Å

Compound M5n with an encouraging docking energy -9.8 kcal/mol occupied the active site of the Enoyl-[acyl-carrier-protein] reductase. It developed hydrogen interaction with nitro group of phenyl ring by Lys165, carbonyl group of anilide by Ile21 and Ala22 and with nitrogen of anilide group by Gly14 and Ser94. Also, both phenyl ring showed π-sigma and π-alkyl interaction with Ile21, Ile95 and Ile16. Pyrazole ring showed π-sigma interaction by Ile16 while alkyl interaction by Ala198 with trimethyl group attached to pyrazole ring (Figure 2). All the docking score and interactions of compounds with amino acids are listed in the table 3.

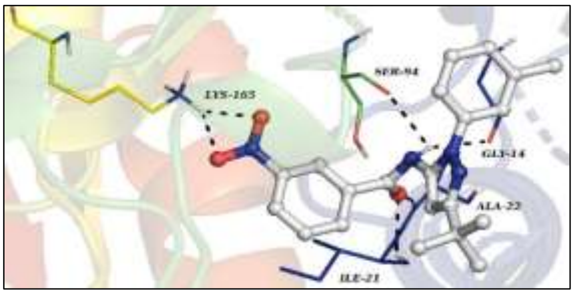

Figure 3: Docked complex of M5n with 4DRE

Compound M5g with the encouraging docking energy -9.6 kcal/mol occupied the site of the Enoyl-[acyl-carrier-protein] reductase. It developed hydrogen interactions with carbonyl group of anilide by Lys165 as shown in figure 4. π-sigma interaction developed with pyrazole ring by Ile21. Also, both phenyl ring and methyl group of phenyl ring developed π-alkyl and alkyl interaction by Met103, Tye158, Met161 and Met199. π-cation interaction developed by Lys165 with phenyl ring (Figure 4).

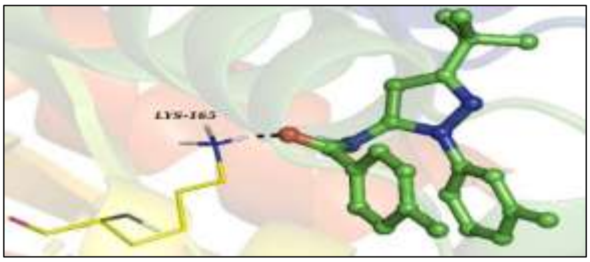

Figure 4: Docked complex of M5g with 4DRE

The compound M5h has docking energy -8.7 kcal/mol housed in the active motif of the Enoyl-[acyl-carrier-protein] reductase and developed the hydrogen interaction with nitrogen of anilide group by Gly14 and with carbonyl group of anilide by Ala22 and Ile21. Also, π-alkyl and alkyl interaction were developed by Ile95 and Ala198 with phenyl ring and trimethyl group attached to another phenyl ring. Pyrazole ring developed π-sigma interaction by Ile16. (Figure 5)

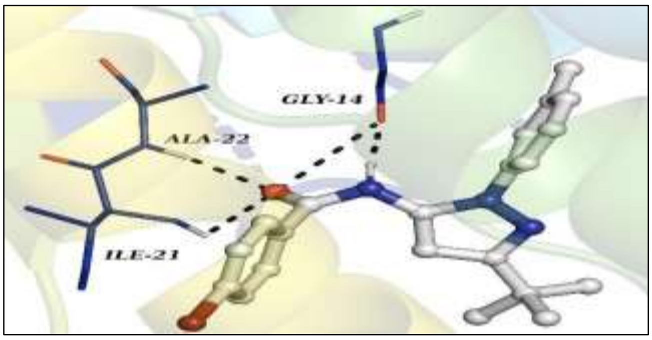

Figure 5: Docked complex of M5h with 4DRE

The compound M5e with docking energies -7.7 kcal/mol occupied the site of the Enoyl-[acyl-carrier-protein] reductase and developed hydrogen interaction with carbonyl group of anilide by Asp148 and Lys165. Phenyl ring developed π-alkyl and π-π stacked interaction by Ile21 and Phe149. Also, bromine group of phenyl ring developed alkyl interaction by Met199, Ile202 and Tyr158. Unfavorable donor- donor interaction was developed by Lys165 with anilide group (Figure 6).

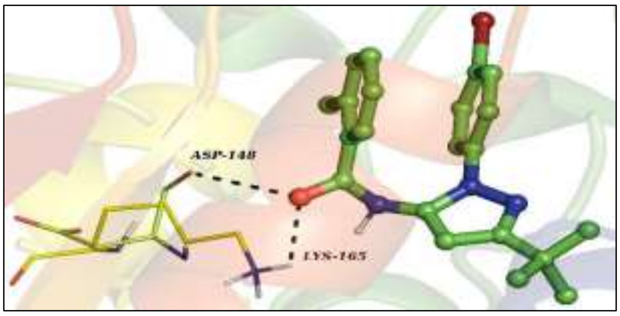

Figure 6: Docked complex of M5e with 4DRE

The compound M5l with docking energies -7.4 kcal/mol occupied the site of the Enoyl-[acyl-carrier-protein] reductase and developed hydrogen interactions with carbonyl group of anilide by Gly96 and Ser94. Both phenyl ring showed π-alkyl and alkyl interaction by Val65, Ile122, Ile95 and Ala198. Phe41 showed π- π stacked interaction with phenyl ring while trifluoromethyl group of another phenyl ring developed halogen (fluorine) interaction by Gly14 and Ser94. Pyrazole ring and trimethyl group of pyrazole ring developed π-sigma and alkyl interaction by Ile16 (Figure 7).

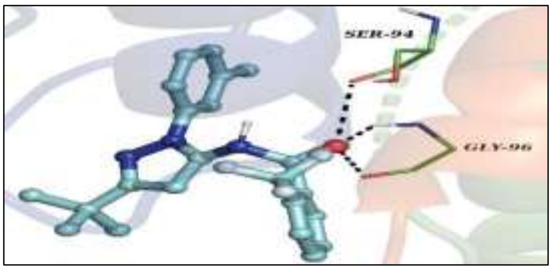

Figure 7: Docked complex of M5l with 4DRE

Table 3: Molecular interaction data and docking energies of the molecules

Comp.	Score*	Hydrogen bond interaction	Hydrophobic and electrostatic contacts
# (NAI)	-10.5	Gly14, Ile21, Ala22, Thr39, Leu63, Gly96, Lys165, Ile194	Ser13, Ile15, Ser19, Ile21, Asp64, Ser94, Gly96, Phe97, Ile122, Met147, Asp148, Phe149, Tyr158, Met161, Ala191, Gly192, Pro193, Thr196, Met199

M5a	-7.8	Ser94, Gly96	Gly14, Ile16, Ser20, Ile21, Phe41, Ser94, Ile95, Phe97, Ile122, Lys165
M5b	-8.5	Gly14, Ile21, Ala22	Ser20, Val65, Ser94, Gly96, Met147, Thr196
M5c	-8.1	Ser94, Gly96	Gly14, Ile16, Ile21, Phe41, Ser94, Ile95, Phe97, Ile122
M5d	-8.8	Gly96	Gly14, Asp42, Arg43, Asp64, Phe97, Thr196
M5e	-7.7	Asp148, Lys165	Gly14, Ser20, Ile21, Ala22, Ser94, Gly96, Met103, Met147, Asp148, Met161, Gly192, Pro193, Ile194, Thr196
M5f	-9.4	Gly96	Gly14, Asp42, Arg43, Gln66, Phe97, Thr196
M5g	-9.6	Lys165	Gly14, Ile16, Ile21, Ala22, Ser94, Gly96, Met147, Phe149, Pro193, Ile194, Thr196, Ala198, Ile202
M5h	-8.7	Gly14, Ile21, Ala22	Ile15, Ser20, Gly40, Phe41, Ser94, Gly96, Met147, Phe149, Lys165, Thr196
M5i	-7.7	Gly14, Ile21, Ala22	Ile15, Ser20, Gly40, Phe41, Ser94, Gly96, Met147, Lys165, Ile194, Thr196
M5j	-8.1	Asp148, Lys165	Ser20, Ile21, Ser94, Gly96, Asp148, Gly192, Pro193, Ile194, Thr196,
M5k	-9.2	Gly14, Ile21, Ala22	Ile15, Ser20, Gly40, Phe41, Ile47, Gly96, Met147, Lys165, Thr196, Leu197
M5l	-7.4	Ser94, Gly96	Ala22, Phe97, Thr196
M5m	-8.3	Asp148, Lys165	Ser20, Ile21, Ser94, Gly96, Met147, Asp148, Gly192, Pro193, Ile194, Thr196
M5n	-9.8	Gly14, Ile21, Ala22, Ser94, Lys165	Ile15, Thr17, Ser20, Gly40, Phe41, Ile47, Gly96, Met147, Asp148, Lys168, Thr196
M5o	-9.2	Gly14, Ile21, Ala22, Ile95	Ile15, Ser20, Gly40, Phe41, Ile47, Ser94, Gly96, Met147, Lys165, Thr196, Leu197

*Kcal/mol, # Co-crystal ligand

5. Conclusion:

In conclusion, the synthesized pyrazole benzamides (M5a–o) exhibited remarkable antibacterial, antifungal, and anti-tubercular activities. Among them, M5i demonstrated the most potent antibacterial effect (MIC: 3.12 µg/mL), while M5b was effective against Bacillus subtilis (MIC: 6.25 µg/ml), with both M5i and M5b also inhibiting Staphylococcus aureus (MIC: 6.25 µg/ml). M5n showed superior activity against Klebsiella pneumoniae (MIC: 6.25 µg/ml), outperforming reference compound 5w. For antifungal efficacy, M5e was the most effective (MIC: 3.12 µg/ml) against Aspergillus flavus and also inhibited Candida albicans (MIC: 6.25 µg/ml). M5k (MIC: 3.12 µg/ml) and M5d (MIC: 6.25 µg/ml) exhibited significant activity against MRSA, with M5k additionally targeting VRSA (MIC: 6.25 µg/ml). M5n further inhibited Enterococcus faecium (MIC: 6.25 µg/ml). Notably, compounds M5i, M5n, and M5b displayed strong anti-tubercular activity (MIC: 6.25 µg/ml) against Mycobacterium tuberculosis, surpassing compound 5w.

Molecular docking studies highlighted M5n and M5g as particularly promising candidates, exhibiting favorable docking energies and robust interactions with Enoyl-[acyl-carrier-protein] reductase (4DRE). These interactions involved key residues, including Lys165, Gly14, Ser94, and Ile21, through hydrogen bonding and π-interactions, suggesting their potential as effective enzyme inhibitors. The comprehensive biological activity and strong molecular interactions indicate that M5n and M5g hold significant promise for further development as therapeutic agents.

References

[1] Salam MA, Al-Amin MY, Salam MT, Pawar JS, Akhter N, Rabaan AA, Alqumber MA. Antimicrobial resistance: a growing serious threat for global public health. In Healthcare 2023; 11(13): 1946. doi: 10.3390/healthcare11131946, MDPI.

[2] Uddin TM, Chakraborty AJ, Khusro A, Zidan BR, Mitra S, Emran TB, Dhama K, Ripon MK, Gajdács M, Sahibzada MU, Hossain MJ. Antibiotic resistance in microbes: history, mechanisms, therapeutic strategies, and future prospects. Journal of infection and public health. 2021; 14(12): 1750-66. doi: 10.1016/j.jiph.2021.10.020

[3] Cong Y, Yang S, Rao X. Vancomycin-resistant Staphylococcus aureus infections: A review of case updating and clinical features. Journal of advanced research. 2020; (21): 169-76. doi: 10.1016/j.jare.2019.10.005

[4] Mancuso G, Midiri A, Gerace E, Biondo C. Bacterial antibiotic resistance: The most critical pathogens. Pathogens. 2021; 10(10): 1310. https://doi.org/10.3390/pathogens10101310

[5] World Health Organization. WHO consolidated guidelines on tuberculosis. Module 4: treatment-drug-resistant tuberculosis treatment, 2022 update. World Health Organization; 2022.

[6] Hoagland DT, Liu J, Lee RB, Lee RE. New agents for the treatment of drug-resistant Mycobacterium tuberculosis. Advanced drug delivery reviews. 2016; (102): 55-72. doi: 10.1016/j.addr.2016.04.026

[7] Drew, R.H.; Isoniazid: An overview, Author: Literature review current through 2023. This topic was last updated: on Dec 13, 2023.

[8] Ethionamide. Available from: https://en.wikipedia.org/wiki/Ethionamide

[9] Padmini T, Bhikshapathi D, Suresh K, Kulkarni R, Kamal BR. Novel aminopyrazole tagged hydrazones as anti-tubercular agents: synthesis and molecular docking studies. Medicinal Chemistry. 2021; 17(4): 344-51. doi: 10.2174/1573406416666200514084747

[10] Kompis IM, Islam K, Then RL. DNA and RNA synthesis: antifolates. Chemical reviews. 2005; 105(2): 593-620. doi:

10.1021/cr0301144, PMID: 15700958

[11] Kulkarni R, Babu H, Kumar K, Gaddam N, Fatima A, Muvvala S, DVRN B, Garlapati A, Vishnav J, Gurav P. Synthesis, antibacterial, antifungal and antitubercular activities of N-pyrazolyl benzamide derivatives. Medicinal Chemistry. 2014; 10(2): 220-27

[12] Kulkarni R, Mitkari U, Achaiah G, Laufer S, Bikshapti DV, Chandrashekar VM, Gurav PB, Joshi SJ, Chipade VD. Substituted benzamides from anti-inflammatory and p38 kinase inhibitors to antitubercular activity: design, synthesis, and screening. Mini-Reviews in Medicinal Chemistry. 2018; 18(17): 1486-97. doi: 10.2174/1389557517666170707105416]

[13] Fatima A, Kulkarni R, Mantipragada B. Design, synthesis, antimicrobial and anti-inflammatory activity of N-pyrazolyl benzamide derivatives. Medicinal chemistry. 2015; 5(12): 521-27. doi: 10.4172/2161-0444.1000311

[14] Ganesh A, Bikshapathi D, Kulkarni R. Pyrazolyl benzamides: synthesis, characterization, and potent biological activity, Part 2. Current Enzyme Inhibition. 2018; 14(1): 26-35(10). doi: 10.2174/1573408013666170516143419

[15] Naim MJ, Alam O, Nawaz F, Alam MJ, Alam P. Status of pyrazole and its biological activities. Journal of Pharmacy and Bioallied Sciences. 2016; 8(1): 2-17. doi: 10.4103/0975-7406.171694

[16] Hunsberger IM, Shaw ER, Fugger J, Ketcham R, Lednicer D. The preparation of substituted hydrazines. IV. Arylhydrazines via conventional methods. J Org Chem. 1956;21(4).

[17] Aasiya Chowdhary, Khandekar Mangala, Chandrashekar VM, Kulkarni Ravindra. Anti-Inflammatory Activities of Pyrazole Benzamides Integrating in Vivo, Molecular Docking, and Dynamics Studies. African Journal of Biomedical Research. 2024, 27(3), 4619-4628.

[18] Andrews JM. Determination of minimum inhibitory concentrations. Journal of Antimicrobial Chemotherapy. 2001; 48(suppl_1): 5-16. doi: org/10.1093/jac/48.suppl_1.

[19] Kowalska-Krochmal B, Dudek-Wicher R. The minimum inhibitory concentration of antibiotics: Methods, interpretation, clinical relevance. Pathogens. 2021; 10(2): 165. doi:10.3390/pathogens10020165

[20] Alqahtani JM, Asaad AM. Anti-tuberculous drugs and susceptibility testing methods: current knowledge and future challenges. J Mycobac Dis. 2014; 4(140): ISSN: 2161-1068. 1-6. doi:10.4172/2161-1068.1000140

[21] Ericsson HM, Sherris JC. Antibiotic sensitivity testing. Report of an international collaborative study. Acta pathologica et microbiologica scandinavica. 1971(Suppl_217)

[22] Zhou W, Yang B, Zou Y, Rahman K, Cao X, Lei Y, Lai R, Fu ZF, Chen X, Cao G. Screening of Compounds for Anti-tuberculosis Activity, and in vitro and in vivo Evaluation of Potential Candidates. Frontiers in Microbiology. 2021; (12). doi: 10.3389/fmicb.2021.658637

[23] Cosconati S, Forli S, Perryman AL, Harris R, Goodsell DS, Olson AJ. Virtual Screening with AutoDock: Theory and Practice. Expert Opin Drug Discov. 2010 Jun 1;5(6):597-607. doi: 10.1517/17460441.2010.484460. PMID: 21532931; PMCID: PMC3083070

[24] Forli S, Huey R, Pique ME, Sanner MF, Goodsell DS, Olson AJ. Computational protein-ligand docking and virtual drug screening with the AutoDock suite. Nat Protoc. 2016 May;11(5):905-19. doi: 10.1038/nprot.2016.051. Epub 2016 Apr 14. PMID: 27077332; PMCID: PMC4868550

[25] Dassault Syst_emes. (2020). BIOVIA Discovery Studio version 4.5. https://www.3ds.com

[26] S. Rosignoli, A. Paiardini, Biomolecules., 12(12), 1764 (2022)